SOLVING THE PERVASIVE PROBLEM OF PROTOCOL NON-COMPLIANCE IN MRI USING AN OPEN-SOURCE TOOL *mrQA*

A PREPRINT

Harsh Sinha[1] and Pradeep Reddy Raamana[1,2,3]

[1]Intelligent Systems Program, School of Computing and Information, University of Pittsburgh
[2]Department of Biomedical Informatics, University of Pittsburgh
[3]Department of Radiology, University of Pittsburgh
{harsh.sinha,raamanap}@pitt.edu

July 17, 2023

ABSTRACT

Pooling data across diverse sources acquired by multisite consortia requires compliance with a predefined reference protocol i.e., ensuring different sites and scanners for a given project have used identical or compatible MR physics parameter values. Traditionally, this has been an arduous and manual process due to difficulties in working with the complicated DICOM standard and lack of resources allocated towards protocol compliance. Moreover, issues of protocol compliance is often overlooked for lack of realization that parameter values are routinely improvised/modified locally at various sites. The inconsistencies in acquisition protocols can reduce SNR, statistical power, and in the worst case, may invalidate the results altogether. We developed an open-source tool called mrQA to automatically assess protocol compliance on standard dataset formats such as DICOM and BIDS, and study the patterns of non-compliance in over 20 open neuroimaging datasets, including the large ABCD study. We demonstrate that the lack of compliance is rather pervasive. The frequent sources of non-compliance include but not limited to deviations in Repetition Time (TR), Echo Time (TE), Flip Angle (FA), and Phase Encoding Direction (PED). We also noticed that GE and Philips scanners exhibited higher rates of non-compliance relative to the Siemens scanners in the ABCD dataset. We strongly recommend continuous monitoring of datasets for protocol compliance before any pre- or post-processing, ideally right after the acquisition, to avoid the silent propagation of severe/subtle issues. While we focus our analysis on neuroimaging datasets, our tool mrQA is domain-agnostic and can work with any DICOM-based datasets.

Keywords DICOM · quality assurance · dataset integrity · protocol compliance · neuroimaging · BIDS

1 Introduction

Large-scale neuroimaging datasets play an essential role in characterizing brain-behavior relationships. The average sample size of neuroimaging studies has grown tremendously over the past two decades [1, 2]. Open datasets like the Alzheimer's Disease Neuroimaging Initiative (ADNI) consists of 800 subjects from 50 sites across the United States collected over 2-3 years [3], the Human Connectome Project (HCP) [4] contains 1200 subjects, the Adolescent Brain Cognitive Development (ABCD) study [5] includes over 12000 subjects at 21 sites, the Autism Brain Imaging Data Exchange (ABIDE) provides a dataset of 1000 individuals at 16 international sites, and the UK Biobank is following about 500,000 subjects in the UK. These large-scale datasets are acquired over several years, involving multiple sites, with several vendor-specific scanner models.

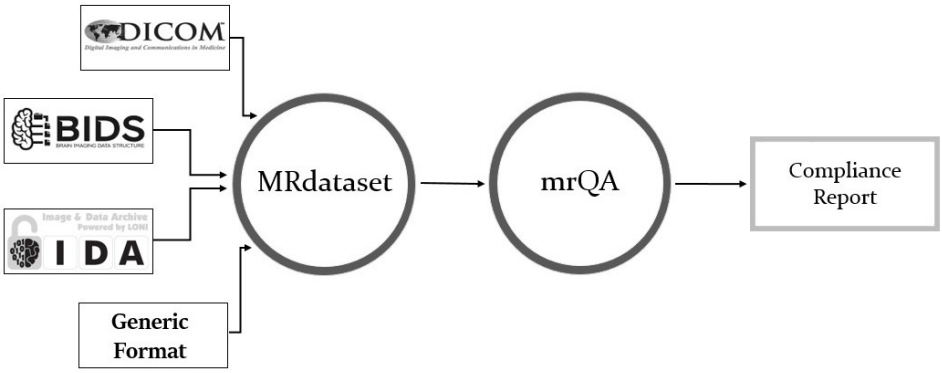

Figure 1: *MRdataset* offers a unified interface to parse & traverse different dataset formats and access acquisition information and metadata e.g. various modalities, subjects, and sessions. This interface is used for generating protocol compliance reports via *mrQA*.

A typical MR imaging session consists of multiple modalities (including but not limited to anatomical, functional, and diffusion MRI) along with their corresponding field maps, localizers, and the like for each subject. Imaging data from these modalities provides complementary information about the structural and functional organization. The electronic protocol files generated by scanners (*i.e.*, Exam Card - Philips, Protocol Exchange - GE, or .exar file - Siemens) include thousands of parameter values for a single session. To use these distinct modalities effectively, it is important to validate the combinations of protocols used for acquisition *i.e.*, evaluating the reliability of chosen imaging sequences and ensuring that the imaging data is acquired accurately for each subject across all sites and scanners. Neither is it a recommended scientific practice nor is it practical to "hope" for data integrity by manual compliance checks across numerous parameters, given the ever-increasing size of neuroimaging studies, cross-site evaluations, multiple scanners, and varied environments.

As maintenance of imaging protocols in MRI centers is typically an ad-hoc and error-prone process, it often leads to variations in acquisition parameters across different subjects and sessions. For instance, protocol configurations are manually uploaded on each scanner which impacts consistency. Inconsistencies arising from software updates and hardware upgrades which alter the default behavior and setting of the scanning interface should be promptly addressed before the MR acquisition. Even subtle deviations in acquisition parameters can potentially affect the reproducibility of MRI-based brain-behavior studies [6]. Prior works have focused on developing post-processing techniques to reduce the impact of such deviations on neuroanatomical estimates [7, 8, 9, 10, 11, 12]. Such post-processing techniques often rely on a large sample size per site to estimate site-specific effects. Recent work by George *et al*. [13] used power analysis techniques to demonstrate that using standardized protocols yields over a two-fold decrease in variability for cortical thickness estimates when compared against non-standardized acquisitions. Therefore, adherence to standardized image acquisition protocols at the scanner is essential for ensuring the quality of MRI-based neuroimaging studies [14, 15]. Otherwise, some subject-specific scans might have to be discarded due to a flawed data collection process, thus reducing the sample size and, consequently, the power of statistical analysis [16]. Yet not much effort has been devoted to eliminating these inconsistencies in image acquisition protocol.

Insufficient monitoring can lead to non-compliance in imaging acquisition parameters, including but not limited to flip angle (FA), repetition time (TR), phase encoding direction (PED), sampling bandwidth, and echo time (TE). This problem becomes particularly relevant for analyses from T1/T2 weighted images, which are known to be sensitive to acquisition parameters [17]. In EPI, co-registration with its structural counterpart becomes difficult if EPI is non-compliant with the field map regarding field-of-view, pixel bandwidth, and multi-slice mode [18, 19]. In DTI, the images acquired with different polarities of PED cannot be used synonymously as they differ in fractional anisotropy estimates [20]. Inconsistencies in image acquisition parameters may implicitly bias the texture in brain images, confounding brain-behavior prediction or phenotypes from brain images [21]. Thus, any analyses conducted without eliminating sources of error in acquisition parameters may reduce statistical power and, in the worst case, may invalidate results altogether, hindering widespread clinical adoption of the experimental results.

Therefore, we present *mrQA* (and *MRdataset*), a software platform to ensure data integrity in MRI datasets. *mrQA* is designed to aggregate and summarize compliance checks on DICOM images at the MRI scanner itself. Automating the compliance check process, *mrQA* can help reduce the risk of errors and omissions in handling and use of DICOM images. DICOM images have an inherent complex structure, and relying on manual interpretation of DICOM fields

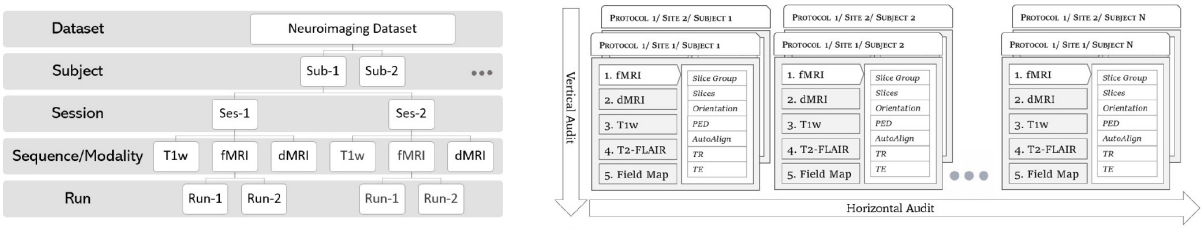

(a) Illustration of hierarchical structure for representing elements of a neuroimaging dataset.

(b) Overview of the relationship between various elements (such as subject, modality, & site) for protocol compliance checks.

Figure 2: *MRdataset* parses the acquisition parameters for all modalities, subjects, sessions, and runs directly from DICOM headers. Neither does it depend on filename hierarchy nor it expects a particular file organization on disk to accommodate varied configurations in MRI datasets. Then, the parameter values are aggregated to assess protocol compliance for a neuroimaging dataset. We define a horizontal audit to be across all subjects in a given modality (compliant w.r.t a predefined protocol), whereas vertical audit checks if a single subject is compliant across all the acquired modalities.

is prone to error. For instance, left-right flips are not easy to spot visually, but they can be verified using automated checks [22]. Such subtle errors can have serious consequences, especially for brain surgery. Prior works [23] have proposed validation of acquisition parameters for BIDS datasets. Their work is focused on the execution of BIDS-apps by identifying variations in acquisition parameters. In contrast, *mrQA* focuses on enunciating variation in acquisition parameters for DICOM images. Even though the DICOM format suffers from storage overhead, with complex specifications, DICOM contains complete acquisition metadata with standardized tags. Therefore, it has been the established output format for medical images. In contrast, NIfTI has limited scope for adding important acquisition parameters in the header. The NIfTI format relies on JSON sidecars for storing important acquisition parameters. *mrQA* can discover variations in acquisition parameters in the rawest data format available, i.e. DICOM format.

mrQA has been developed primarily for DICOM-based datasets, but it also expands its functionality to NIfTI-based BIDS datasets. It is important to note that reformatting/validation of BIDS datasets typically occurs years after the data acquisition process has been completed. When non-compliant scans are discovered at a later stage, researchers may have to exclude such subjects/sessions to maintain the reliability of their findings. Therefore, it is important to embrace a mindset of proactive quality assurance i.e. validating the acquired data as soon as possible to prevent any inconsistencies in acquisition. We recommend checking the imaging acquisition parameters for compliance based on DICOM files as soon as possible either during or immediately after the scan. It might be possible that the default acquisition parameters in the scanning interface are inconsistent with the recommended protocol. In the broader scope,

```python
# programmatic interface in Python
from MRdataset import import_dataset
from mrQA import check_compliance

dicom_ds = import_dataset(data_source='/path/data', ds_format='dicom', name='abc')
check_compliance(dicom_dataset)
# In [1]: In abc dataset, modalities "GRE, DTI, rsfMRI" are non-compliant. See
↪  abc_DATE_09_07_2022_17_07.html for report

bids_ds = import_dataset(data_source='/path/to/data', ds_format='bids', name='xyz')
check_compliance(bids_dataset)
# In [2]:  In xyz dataset, modalities "func" are non-compliant. See
↪  xyz_DATE_09_07_2022_17_07.html for report
```

```bash
# command line interface in bash
$ mrqa --data-source /path/to/dataset --format bids --name my_bids_dataset
```

Listing 1: Two different ways of using *mrQA* to generate a compliance report.

mrQA enables researchers to enforce strict acquisition protocols to alleviate unintended sources of error at their first step of the data acquisition system. Moreover, *mrQA* can be set up as a continuous monitoring service (daily, hourly, or real-time) for aggregating compliance checks on DICOM images.

To summarize, a critical aspect of MR imaging is adherence to the recommended protocol which would enhance the validity and consistency of acquired images. Secondly, inconsistencies should be checked promptly so that corrective measures can be taken to minimize differences in acquisition parameters over the entire project timeline. Finally, checking for compliance would make us much more familiar with our own data, enabling us to draw meaningful conclusions while considering potential biases, confounds, or anomalies that impact the quality of statistical analysis.

In addition, we provide a critical perspective on the wide diversity of acquisition metadata in open neuroimaging datasets. The motivation behind this exploration is to identify the common parameters which are prone to change. By understanding common issues, we can be more attentive to these parameters during the acquisition. It is important to note that the exploration of common issues in acquisition is not about finger-pointing for mistakes. Rather, it is about recognizing common issues of non-compliance and working collaboratively to address them. Towards this end, we assess protocol compliance, or lack thereof, in the The Adolescent Brain Cognitive Development (ABCD) Study dataset [24], over 20 datasets on OpenNeuro [25] and public DICOM datasets on The Cancer Imaging Archive (TCIA) [26]. We also discuss common sources of non-compliance and their impact on image quality and downstream statistical analyses.

2 Methods

The proposed framework aims to help researchers monitor compliance in neuroimaging datasets. The execution of the entire framework is depicted in two stages, namely *MRdataset* and *mrQA* as shown in Figure 1. First, we parse the input dataset to create a data structure that stores the acquisition parameters of all the modalities, subjects, and sessions in a neuroimaging study (via *MRdataset*). Then, the acquisition parameters are aggregated and summarized for generating a protocol compliance report (*mrQA*). The framework allows researchers to discover deviations in scanning parameters and fix critical errors regardless of the dataset format and folder structure on disk. This section includes a detailed description of the methods, along with the design and API specifications. The source code is publicly available at `https://github.com/Open-Minds-Lab/MRdataset` and `https://github.com/Open-Minds-Lab/mrQA`.

2.1 Creating a unified interface *(MRdataset)*

Experimental neuroimaging data is hugely diverse and may be structured differently according to study design or clinical protocol, especially the stimulus, behavioral response, and interventions. Thus, any tool must address the fundamental capability of representing and manipulating common dataset formats. *MRdataset* provides a unified interface to simplify the traversal of neuroimaging datasets by adopting modular classes for each dataset format as well as different levels in the hierarchy, such as modalities, subjects, sessions, and runs [27] as shown in Figure 2. *MRdataset* infers information about the hierarchical structure directly from the DICOM headers. *MRdataset* doesn't rely on filenames or expect a particular idiosyncratic organization of files to process various configurations. It provides a simple modular interface to improve the use and accessibility of neuroimaging datasets.

MRdataset provides a consistent set of methods for data access irrespective of the dataset format (such as BIDS, and DICOM). In the future, we expect to extend the *MRdataset* dataset class to support other data formats, such as LONI IDA, but these were not included in the initial design. In addition to the desired unified interface, *MRdataset* performs basic validation to reject localizers, head scouts, and phantoms. Keeping these considerations in mind, the package is written in Python, and it uses *pydicom* [28] for reading DICOM images. Python is becoming the de facto standard for scientific applications as it provides community support and easy extensibility for the future [29].

2.2 Generating a compliance report *(mrQA)*

In this section, we describe the considerations and the procedure used for evaluating protocol compliance of an MR imaging dataset. There can be two kinds of compliance evaluations - a *horizontal audit* and a *vertical audit*. Both of these evaluations are important to establish data integrity.

A *horizontal audit* is focused on investigating parameters across all subjects in a neuroimaging dataset. In a *horizontal audit*, a run is said to be *compliant* if the acquisition parameters for the run are the same as the reference protocol. A reference protocol is a pre-defined set of values for each of the acquisition parameters. As shown in Figure 2, a subject may have one or more sessions for each modality (e.g. T1, T2) and each session has multiple runs. A subject is said to be *compliant* for a given modality if all the sessions for the subject are *compliant* with the reference protocol. Therefore,

a subject can be *compliant* for one modality (say T1w), but it might be *non-compliant* for another modality (say T2w). A subject is tagged as *non-compliant* even if a single run is found to be non-compliant for a given modality. Similarly, a modality is said to be *compliant* if all the subjects in this modality are *compliant* for all sessions. This means there might be some datasets where none of the subjects are compliant.

A *horizontal audit* is essential to ensure the acquisitions across sessions were performed correctly. However, a *horizontal audit* does not address the interaction between multiple modalities within a given session. In contrast, a *vertical audit* checks for compliance issues across all the modalities for a single imaging session. For example, given a subject, all field maps must be set up with the same field-of-view, pixel bandwidth, and multi-slice mode as the probe [18]. Similarly, optimization of homogeneity for the magnetic field, known as shimming, is specific to a subject. The shimming method should not vary across modalities for a single subject. It is ideal to have consistent shimming, especially for spectroscopic experiments [30] even though subtle deviations in shimming might not pose a critical problem. In addition, vertical audits are also helpful in revealing specific scans which are found to be non-compliant across multiple modalities. For instance, a vertical audit can spot navigator slices that might have been erroneously uploaded along with a scan for a subject. We recommend that both *horizontal audit* and *vertical audit* must be enforced to eliminate subtle errors in acquisition protocols.

Further, we advocate a two-pronged approach for checking compliance against a reference protocol. The first is *pre-acquisition* compliance, where the parameters will be checked for compliance against a reference protocol before a scan is performed. And the second step is *post-acquisition* compliance, where the parameters are checked after complete data acquisition across all subjects, validating the *acquired* dataset for compliance. Ideally, both of these two prongs should be performed to maximize data integrity and minimize loss i.e. carrying out pre-acquisition compliance checks at initial setup to prevent bad acquisitions in the first place and validating the acquired images with post-acquisition compliance checks to remove any accidental or unknown sources of non-compliance.

In this work, we focus on the horizontal audit via post-acquisition compliance to assess neuroimaging datasets for compliance. Assuming that acquisition for most subjects in a given study follows a predefined recommended protocol, *mrQA* infers the most frequent values for each parameter within a modality to construct the *reference protocol*. Then for each subject in the modality, *mrQA* compares the parameter values of each run with this *reference protocol* to determine whether the subject is non-compliant. Finally, each modality is indicated with scores of non-compliance and compliance percentage as shown in Equation 2. Note that multi-echo sequences will have a reference protocol with multiple echo times. Therefore, the runs in each sequence are stratified by echo time before inferring the most frequent values for each parameter.

$$\begin{aligned} \text{non-compliant } \% &= \frac{\text{Number of non-compliant subjects in modality}}{\text{Total number of subjects in modality}} \times 100 \\ \text{compliant } \% &= 100 - \text{non-compliant } \% \end{aligned} \tag{1}$$

```python
from MRdataset import import_dataset
from mrQA import check_compliance

dicom_ds = import_dataset(data_source='/path/data', ds_format='dicom', name='abc')
check_compliance(dicom_dataset)
# In [1]: In abc dataset, modalities "GRE, DTI, rsfMRI" are non-compliant. See
↪  abc_DATE_09_07_2022_17_07.html for report

bids_ds = import_dataset(data_source='/path/to/data', ds_format='bids', name='xyz')
check_compliance(bids_dataset)
# In [2]:  In xyz dataset, modalities "func" are non-compliant. See
↪  xyz_DATE_09_07_2022_17_07.html for report
```

```bash
$ mrqa --data-source /path/to/dataset --format bids --name my_bids_dataset
```

Listing 2: An example using *mrQA* (above: Python API, below: CLI) for generating a compliance report.

(a) Example of a reference protocol.

Scanning Sequence	Echo Train Length	Phase Encoding Direction	Magnetic Field Strength	Phase Encoding Direction	Multi Slice Mode	Pixel Bandwidth	Flip Angle	MR Acquisition Type
GR	1	j	3	ROW	interleaved	350	40	2D
is3D	**Phase Encoding Steps**	**Shim**	**Repetition Time**	**iPAT**	**Manufacturer**	**Sequence Variant**	**Body Part Examined**	**Echo Time**
False	448	Standard	465	Grappa	SIEMENS	MTC_SS	BRAIN	3.73

(b) Summary of non-compliance for a toy dataset.

Modality	Non-compliant		Non-compliant subjects	Reasons	Compliant		Total subjects
rsfMRI	0	0.00 %			5	100.00 %	5
GRE	1	20.00 %	sub-566	Pixel Bandwidth	4	80.00 %	5
T2-FLAIR	0	0.00 %			5	100.00 %	5
DTI	1	20.00 %	sub-879	Phase Encoding Direction	4	80.00 %	5
T1-weighted	0	0.00 %			5	100.00 %	5
SWI	0	0.00 %			5	100.00 %	5

(c) Detailed report for non-compliance in GRE modality

Parameter	Ref. Value	Found	Subject_Session
PixelBandwidth	350	485	sub-566_6, sub-566_7, sub-566_8, sub-566_9, sub-566_10

Table 1: (a) An example reference protocol, and (b,c) compliance report for a toy neuroimaging dataset. Note that the reference protocol can either be pre-defined or inferred by searching for most frequent values for each parameter. The toy dataset has 7 modalities across 5 subjects. Subjects sub-566 and sub-879 are non-compliant w.r.t Pixel Bandwidth and Phase Encoding Direction respectively. For gradient-echo (GRE) modality, subject *sub-566* has a non-compliant pixel bandwidth for sessions 6-10.

An example script for generating compliance reports is provided in Listing 1. An HTML report is generated for a toy dataset that presents complete information in a concise manner (as shown in Table 1). The report has two parts - a summary view which gives a brief assessment of protocol compliance for all the modalities. Following the summary, each modality is accompanied by a detailed view. There are two non-compliant subjects, *sub-566* and *sub-879*, for the modalities GRE and DTI. Subject *sub-566* has non-compliant pixel bandwidth, while subject *sub-879* has an non-compliant PED. For instance, pixel bandwidth in the reference protocol is 350, but subject *sub-566* has a pixel bandwidth of 485 in sessions 6, 7, 8, 9, and 10. The full report contains reference protocols for each modality and corresponding details about sources of error in acquisition parameters.

$$\text{non-compliant } \% = \frac{\text{Number of non-compliant subjects in modality}}{\text{Total number of subjects in modality}} \times 100$$
$$\text{compliant } \% = 100 - \text{non-compliant } \% \tag{2}$$

```python
from mrQA import monitor
monitor(name='xyz', data_source='/path/data', output_dir='/reports/xyz')
```

```
$ mrqa_monitor --data-source /path/data --name xyz --output-dir /reports/xyz
```

Listing 3: An example of *mrQA* being used for monitoring *xyz* dataset. (above: Python API, below: CLI).

Table 2: The table summarizes the compliance report for DICOM images from ABCD-baseline FastTrack Active series. For each of the modality (i.e. T1, T2 and field maps), the table shows the vendor, the percentage of non-compliant & compliant subjects, and the parameters which were found to be non-compliant i.e. Repetition Time (TR), Echo Time (TE), Flip Angle (FA) and Pixel Bandwidth (PB). Some minor cases were observed in Phase Encoding Direction (PED), Phase Encoding Steps (PES), Echo Train Length (ETL), and Shim. In contrast to scans acquired with Philips and GE, images scanned with Siemens exhibit minimal non-compliance across all the modalities. Ensuring compliance in acquisition parameters manually is non-trivial for large-scale multi-site datasets such as ABCD. Automated tools like mrQA can help researchers achieve protocol compliance in a practical manner.

Modality	Vendor	#Non-compliant Subjects		Total Subjects	Parameters	#Compliant Subjects	
T1	GE	59	2.00 %	2941	TE, TR, PB	2882	97.99 %
	Philips	980	64.43 %	1521	TE, ETL, PED, PES, PB, TR	541	35.56 %
	Siemens	2883	39.96 % †	7214	Shim, TE	4331	60.03 %
T2	GE	907	32.19 %	2817	TE, TR, PB	1910	67.80 %
	Philips	916	62.82 %	1458	TE, PB	542	37.17 %
	Siemens	6	0.08 %	7030	PED, Shim	7024	99.91 %
Diffusion Fmap	GE	620	22.26 %	2785	FA, PB	2165	77.73 %
Diffusion Fmap A≫P	Philips	3	0.20 %	1441	PB	1438	99.79 %
	Siemens	128	1.81 %	7057	PED, TR, Shim	6929	98.18 %
Diffusion Fmap P≫A	Philips	4	0.27 %	1439	PB	1435	99.72 %
	Siemens	233	3.30 %	7053	PED, TR, Shim	6820	96.69 %
fMRI Fmap	GE	0	0.00 %	2862		2862	100.00 %
fMRI Fmap A≫P	Philips	873	58.70 %	1487	FA, PB	614	41.29 %
	Siemens	1	0.01 %	7200	Shim	7199	99.98 %
fMRI Fmap P≫A	Philips	875	58.76 %	1489	FA, PB	614	41.23 %
	Siemens	0	0.00 %	7202		7202	100.00 %

† There are minor deviations in TE (ms) within the range (2.88, 2.9)

2.3 Continuous monitoring for datasets

Apart from generating post-acquisition compliance reports for a neuroimaging study, *mrQA* is being used for continuous monitoring of DICOM datasets in MR labs. *mrQA* has been set up as a cron job to generate reports at regular intervals, such as on a daily or weekly basis. Meanwhile, if new sessions are added to the study, *mrQA* reads the new DICOM files added since the previous run and generates updated compliance reports for the study. The automatic reporting feature is especially useful to notify researchers about any non-compliance in a timely manner so that corrective action can be taken promptly. An example script is provided in Listing 2, which must be executed at regular intervals.

3 Results

We focused on evaluating public datasets as they often serve as a benchmark for neuroimaging analyses. We tested *mrQA* with 20 large BIDS datasets publicly available on OpenNeuro [25]. These datasets on OpenNeuro were chosen based on their large size and availability of JSON sidecar files. The software was tested with public DICOM datasets available on The Cancer Imaging Archive (TCIA) [26] (see Appendix A). Finally, *mrQA* was tested on ABCD FastTrack Active Series which provides a unique opportunity to test on a large and diverse sample of over 11,000 subjects across multiple sites and various scanner models.

The exploration is not meant to be a finger-pointing exercise, rather the availability of these datasets has made it possible to discover common issues of non-compliance in MR acquisition. By understanding these common issues, we can be more attentive to these parameters during acquisition. Assuming that acquisition for most subjects in a given study follows a predefined standardized protocol, the most frequent value for each parameter is taken as the reference value. Table 2 and Table 3 summarize the results for ABCD and OpenNeuro datasets, respectively. Frequent sources of

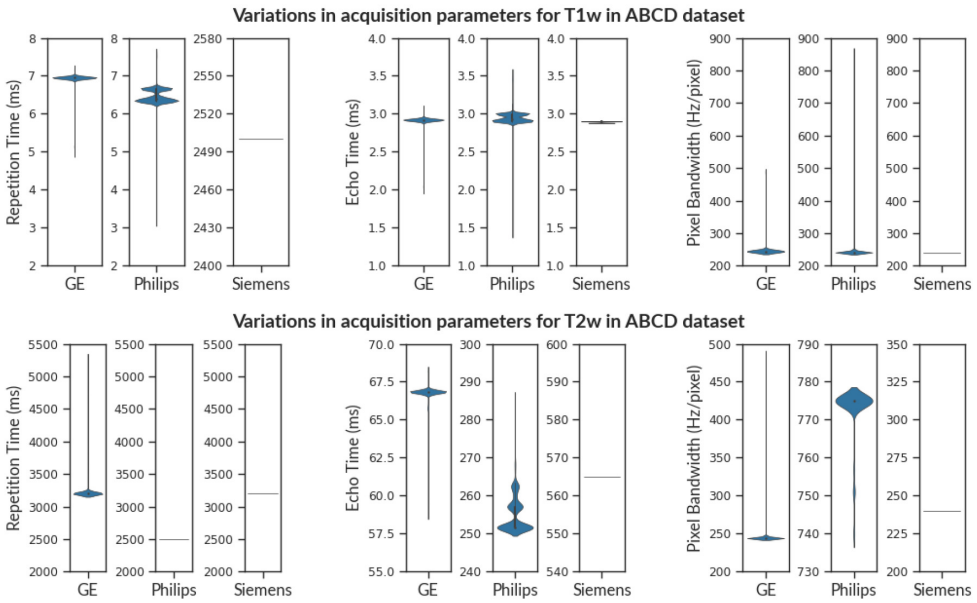

Figure 3: The violin plot shows the variance in Repetition Time (TR), Echo Time (TE), and Pixel Bandwidth (PB) for T1w images (above) and T2w images (below) in the ABCD Dataset. Observe that various vendors have a distinct range of acquisition parameters e.g. Repetition Time (T1w) and Echo Time (T2w). This is because different vendors provide specific imaging sequences e.g. MPRAGE (Siemens) and SPACE(Philips) even though the modality might be the same (T1w). Therefore, checking cross-vendor compliance is non-trivial. Moreover, scans from Siemens have consistent acquisition parameters in contrast to scans from Philips and GE scanners for both T1w and T2w images.

non-compliance include the PED, TR, TE, Flip Angle (FA), and Pixel Bandwidth (PB). The compliance reports are publicly available at `https://github.com/Open-Minds-Lab/mrQA-reports`

3.1 Evaluation of FastTrack Images for ABCD

The Adolescent Brain Cognitive Development (ABCD) [24] is a multi-site longitudinal study focused on understanding the development of the brain in adolescents over a diverse set of socio-demographic features. We analyzed ABCD-baseline scans for three modalities, namely T1-weighted, T2-weighted, and field maps as shown in Table 2. As the objective for *mrQA* is to achieve real-time protocol compliance, we analyze DICOM images from the FastTrack Active Series for each modality. Note we assume that all the data collected so far has been acquired with a single protocol as published in Table 2 in [31] but we are aware that this protocol might have changed slightly over the years for various reasons. As these details are currently not accessible to us during our analysis of the dataset as a whole, we analyzed it as it was shared. If we redo the analyses accounting for such approved intentional changes in the reference protocol, our results are likely to change and we may see different levels of non-compliance. To accommodate such intentional changes, it is best to run *mrQA* on subsets with a single fixed reference protocol for an accurate estimation of non-compliance in the dataset.

We observe that T1w MRI scans from Philips scanners exhibit non-compliance of 64.43%. As shown in Figure 3, the echo-time (TE) varies in the range (1.4 ms, 3.56 ms) for Philips scanners, even though structural scans are not multi-echo in general. Similarly, TR varies in the range (3 ms, 7.63 ms). We also observe some minor issues in PED, Echo Train Length (ETL), Pixel Bandwidth (PB), and Phase Encoding Steps (PES). Similarly, T1w images from the GE scanner have issues of non-compliance in TE, TR, and PB. However, these issues affect 2% of subjects only. In contrast, scans from Siemens scanners exhibit some minor issues in TE and shim. Although echo time varies for 39.96% of the subjects, there are only minor deviations within the range (2.88 ms, 2.9 ms).

Similar to T1w images, we observe that 62.82% of subjects are non-compliant for T2w scans from Philips scanners. Figure 3 shows that TE varies in the range (251.49 ms, 285.23 ms) while PB (Hz/pixel) varies between (740, 775). We observe considerable non-compliance (32.19%) in TE, and TR values from GE scanners for T2w images. TE varies in the range (59.1 ms, 68.2 ms) while TR varies in the range (3200 ms, 5297 ms). In contrast, Siemens scanners exhibit minor issues in PED and shim for only 0.08% of subjects.

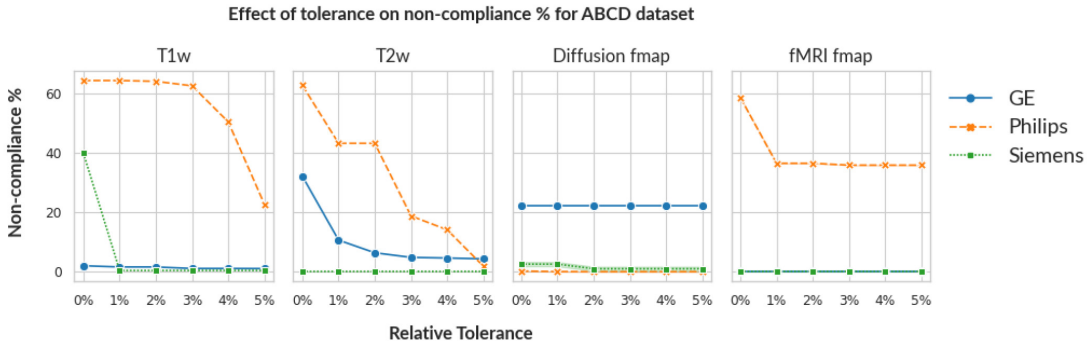

(a) Effect of changing tolerance level for non-compliance in the ABCD-Baseline FastTrack Active Series across scanner vendors. In contrast to Philips and GE, Siemens scanners show minimal non-compliance across all the modalities at a 1% tolerance level.

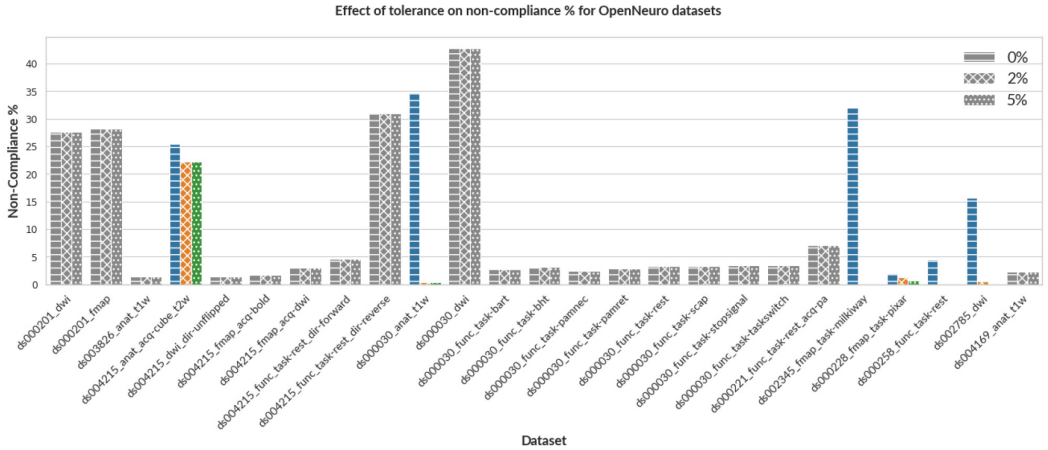

(b) The non-compliance% is not affected by changing the tolerance level for most of OpenNeuro datasets except `ds004215_acq-cube_t2w`, `ds000030_anat_t1w`, `ds002345_task-milkiway`, `ds000228_fmap_task-pixar`, `ds000258_func_task-rest` and `ds002785_dwi` (highlighted in color)

Figure 4: By default, *mrQA* checks for absolute equivalence of parameter values. Given the context of the neuroimaging study, it might be possible to include tolerance in the variation of these acquisition parameters, however, the tolerance level should be best judged by investigators. Note that changing the tolerance level will not affect the non-compliance% if the deviation is too large, or if acquisition parameters are categorical.

Table 2 also shows the assessment of field maps in the ABCD dataset. The subjects are stratified into vendor and PED-specific groups as per information in the DICOM header. Often neuroimaging experiments consist of both A$\gg$P and P$\gg$A scans to reduce artifacts like eddy current effects, and susceptibility artifacts[32]. Therefore, the scans will not have a unique PED across all scans. Note that in the ABCD dataset, Siemens and Philips scanners had distinct fieldmaps each annotated with a PED (AP/PA). However, such annotation was absent in fieldmaps from GE scanners. To avoid misinterpretation, compliance checks should be performed within these sub-groups of A$\gg$P and P$\gg$A scans. Similarly, the field maps intended for Diffusion Images should not be compared to the field maps intended for fMRI images. This information is not automatically captured in DICOM images and should be annotated manually after acquisition. BIDS JSON sidecar has `IntendedFor` parameter which is not automatically exported by *dcm2niix* [33] but can be manually annotated by dataset-specific scripts. We observe that field maps for Diffusion images from GE scanners have a 22.26 % non-compliance due to two distinct values of flip angles i.e. 77° and 90° respectively. Similarly, Philips scanners exhibit non-compliance in flip angle for fMRI field maps. We observe that a lot of subjects have two sessions with flip angle values of 52° and 90°, respectively. The report indicates that these subjects don't comply with a single predefined value for flip angle. We choose to flag this issue, however, whether it is an issue or a study requirement would be best judged by the investigators of the study. We also observe some minor issues in TR and

TE. In contrast, field maps acquired with Siemens scanner have a flip angle of 90°, and some minor issues in Shim, PED, and TR.

As compared to Philips and GE scanners, MRI scans acquired with Siemens scanners are observed to be consistent and compliant achieving more than 99% compliance over seven thousand subjects both in T2w and field maps. We observed that MR scans from Siemens scanners were performed only on Prisma scanners with a consistent software version (*syngo MR E11*). In contrast, scans for Philips were performed on Achieva dStream and Ingenia models, and the GE scans were executed on MR750 and DV25-26. Furthermore, both GE and Philips scans had differences in software versions. The difference in hardware and software versions might have been a potential cause of non-compliance in acquisition parameters for Philips and GE scanners. Our findings are consistent with those reported by the ABCC collection [34]. They observed a relatively high post-processing quality control failure rate, particularly for images derived from GE and Philips scanners.

By default, *mrQA* checks for absolute equivalence of parameter values. Although, absolute equivalence is preferred to minimize incongruities, minor differences in decimal values may not necessarily be a part of the inclusion/exclusion criteria for a subject. Therefore, we analyze the non-compliance percentage in each of these modalities by increasing the tolerance level i.e. increasing the acceptable range of variation in parameter value against the reference value. Figure 4 shows how increasing the relative tolerance level affects the level of non-compliance for T1w, T2w images, and field maps in the ABCD dataset. As described in Table 2, the primary source of non-compliance for T1w and T2w images are TE, TR, and PB. However, for the field maps, the issue is borne from non-compliance in flip angles. For T1w and T2w images, the percentage of non-compliance drops close to zero, indicating that the acquisition parameter had differences within 5% tolerance. However, for field maps, the percentage of non-compliance plateaus at 22.26% for diffusion field maps from GE and 35.91% for fMRI field maps from Philips. This emerges from differences in flip angle as shown in Figure 5.

3.2 Evaluation of BIDS datasets on OpenNeuro

OpenNeuro [25] is a data archive dedicated to open neuroscience data sharing based on FAIR principles [35]. We analyze over 20 open datasets available on OpenNeuro accessible in BIDS format. Table 3 presents some of the datasets which exhibit non-compliance in acquisition parameters. Due to the absence of standard acquisition metadata in NIfTI files, we rely on associated JSON sidecar files for evaluating protocol compliance on NIfTI-based datasets. The most common image acquisition parameters which suffer from variation are repetition time (TR), echo time (TE), PED, flip angle (FA), and magnetic field strength (MFS). Some datasets had distinct data clusters under the same project name. These data clusters can be *repeat experiments* with varying acquisition parameters for each subject e.g. scans with different PED (A≫P, P≫A) for DWI or separate cognitive or behavioral tasks captured with different acquisition protocols in an fMRI study. In such cases, none of the subjects would be seen to comply with a single predefined protocol and compliance checks should be performed after stratification into coherent clusters to avoid misinterpretation. Table 3 shows each of the modalities stratified by entities such as *task* and *acquisition*.

We observed that a lot of subjects in datasets such as `ds002843`, `ds000117`, `ds000228`, `ds001242`, `ds004116`, `ds003647`, and `ds002345` were missing crucial parameters (such as PED, magnetic field strength, echo train length) from their respective JSON sidecar. We observe that each of the OpenNeuro datasets exports a varying set of acquisition parameters because, unlike DICOM tags, the acquisition parameters exported to a JSON sidecar are not standardized. If there is a considerable level of non-compliance, the dataset can be explicitly standardized before it is used for morphometric analyses. However, the standardization would have limited validity due to missing acquisition parameters which might impact the reliability of results. Therefore, we recommend that compliance should be checked using DICOM images, which contain complete acquisition metadata with standardized tags.

We also observe that often the same subjects are tagged as non-compliant across several parameters. This can help in identifying consistent patterns in sources of non-compliance. For example, if the same subject is found to be non-compliant for TR and flip angle in T2w FLAIR sequences, this may indicate that the subject was not comfortable inside the scanner, and therefore SAR was adjusted by reducing flip angle and increasing TR value [36]. Therefore, adequate support may be provided to the particular subject during any further scans to ensure compliance. We found this issue in several datasets such as `ds003826`, `ds004169`, `ds000221`, `ds000030`, `ds000201`, `ds004215`, and `ds000258`. Such patterns might also be helpful in identifying particular sites, or scanners that might be the cause of non-compliance.

Figure 6 provides a visual representation of variance in some of the important acquisition parameters such as echo time, repetition time, pixel bandwidth, and PED across a few OpenNeuro datasets. Each plot shows the distribution of values for the corresponding acquisition parameters, with the width representing the frequency at different levels of each parameter. For each of the violin plots, we observe that the datasets have one or two clusters of values across the

Table 3: The table summarizes compliance report for some OpenNeuro datasets that exhibit deviations in acquisition protocol. For each of these datasets, the table shows the modality, the associated suffix for various tasks/acquisition, the percentage of non-compliant & compliant subjects for each modality, and the parameters which were found to be non-compliant i.e. Repetition Time (TR), Echo Time (TE), and Flip Angle (FA). Some minor cases were observed in Phase Encoding Direction (PED), Phase Encoding Steps (PES), Sequence Variant and Pixel Bandwidth (PB). Thus, mrQA provides the ability to automatically discover scanner-related variance in MR datasets. Automatic compliance checks are especially important for large datasets which exhibit non-compliance rate below 1% because manual/ad-hoc checks are ineffective at detecting these subtle issues.

Dataset	Modality	Differentiating Entities*	Vendor	#Non-Compliant Subjects		Total Subjects	Parameters	#Compliant Subjects	
ds000201	dwi		GE	21	27.63%	76	PB	55	72.36%
	fmap			24	28.23%	85	PED, PB, TR	61	71.76%
ds003826	anat	t1w	Siemens	2	1.47%	136	PES, SV	134	98.52%
ds004215	anat	acq-cube_t2w	GE	39	25.49%	153	TE, TR	114	74.50%
	dwi	dir-unflipped		2	1.39%	143	PB	141	98.60%
	fmap	acq-bold		1	1.69%	59	PED	58	98.30%
	fmap	acq-dwi		2	3.03%	66	PED, PB	64	96.96%
	func	task-rest_dir-forward		6	4.61%	130	FA, PED	124	95.38%
	func	task-rest_dir-reverse		40	31.00%	129	FA, PED	89	68.99%
	perf	asl		1	0.70%	142	TR	141	99.29%
ds000030	anat	t1w	Siemens	92	34.71%†	265	PES, PB	173	65.28%
	dwi			112	42.74%	262	PB, TR	150	57.25%
	func	task-bart		7	2.66%	263	PED	256	97.33%
	func	task-bht		8	3.10%	258	PED	250	96.89%
	func	task-pamnec		5	2.41%	207	PED	202	97.58%
	func	task-pamret		6	2.88%	208	PED	202	97.11%
	func	task-rest		9	3.35%	268	PED	259	96.64%
	func	task-scap		9	3.35%	268	PED	259	96.64%
	func	task-stopsignal		9	3.38%	266	PED	257	96.61%
	func	task-taskswitch		9	3.38%	266	PED	257	96.61%
ds000221	fmap	acq-GE	Siemens	1	0.31%	317	PED	316	99.68%
	fmap	acq-SE		1	0.44%	227	PED	226	99.55%
	func	task-rest_acq-PA		14	7.07%	198	TE	184	92.92 %
ds002345	func	task-milkway	Siemens	17	32.07%†	53	TR	36	67.92 %
ds000228	func	task-pixar	Siemens	3	1.93%	155	FA	152	98.06 %
ds000258	func	task-rest	Siemens	4	4.49%†	85	TR	85	95.50%
ds002785	dwi		Philips	33	15.63%†	211	TR	178	84.36%
ds004169	anat	t1w	Siemens	27	2.24%	1202	FA, PES, PB, TR	1175	97.75%
	func	task-nback		3	0.25%	1189	FA, PED	1186	99.74%
	func	task-rest		2	0.19%	1029	FA, PED	1027	99.80%

† There are minor differences in parameter values. See dicussion.
* For BIDS datasets, entities correspond to an altered acquisition parameter

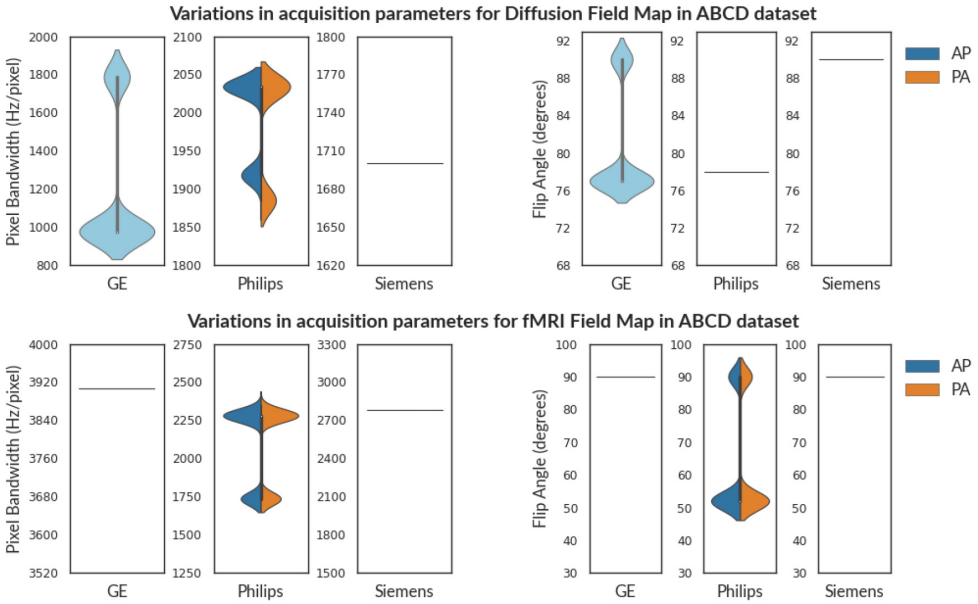

Figure 5: The violin plot shows the variance in Flip Angle(FA) and Pixel Bandwidth (PB) for Diffusion (above) and fMRI (below) field maps in the ABCD Dataset. Siemens and Philips scanners had distinct fieldmaps each annotated with a PED (**AP**/**PA**). However, sequences from GE scanners (denoted by **cyan**) were not annotated in the ABCD dataset. In contrast to scans from Philips and GE scanners, MR scans from Siemens have consistent acquisition parameters across both diffusion and fMRI field maps

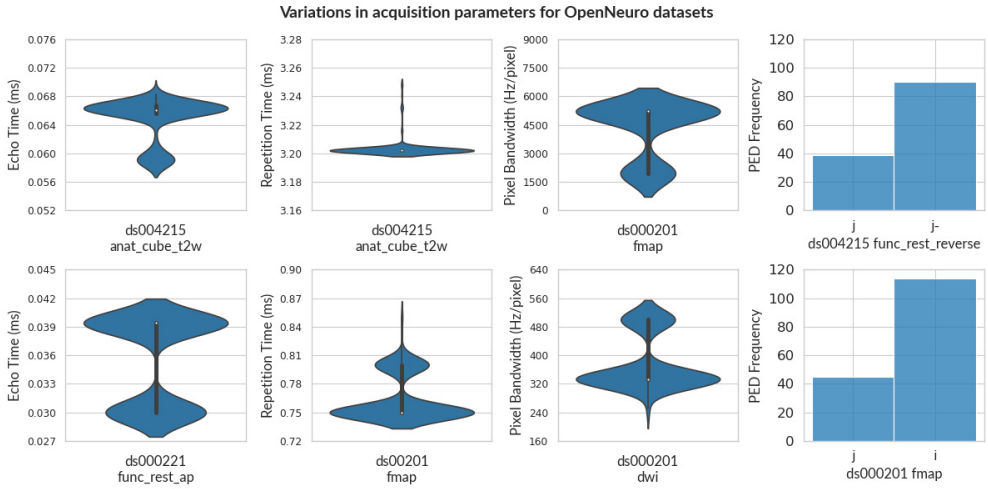

Figure 6: The violin plot shows the variance in Echo Time, Repetition Time, and Pixel Bandwidth for some OpenNeuro Datasets. For violin plots, the width represents the frequency at different levels of each parameter. A histogram chart shows the number of scans for each PED. Note that, even though the entity label specifies PED as *reverse* for `ds004215`, PED is not consistent. This indicates that ensuring compliance is an arduous process, and issues of non-compliance might be overlooked even after careful effort in data acquisition.

dataset. Although it is desirable to have an equal number of scans for PED, as a discrepancy in PED would be reflected by lower fractional anisotropy values, it might not be possible due to the requirements of the study.

Further, we evaluate the non-compliance of each of these datasets after increasing the tolerance level. Figure 4 shows the percentage of non-compliance for some of the OpenNeuro datasets with a tolerance level of 0% (absolute equivalence), 2%, and 5%. We observe that the percentage of non-compliance decreases for 6 datasets only (shown in color), while the percentage of non-compliance for all other datasets is not affected (shown in gray). Changing the tolerance level will not affect the non-compliance percentage if the deviation from the reference is too large, or if the non-compliant parameters are categorical (e.g. PED).

4 Discussion

To obtain better insight into the impact of variation in acquisition parameters on image quality, statistical analyses, and the issue of non-conformance among different vendors in terms of MRI physics parameters, we discuss these issues contextualizing them within the broader literature.

4.1 Effect on image quality

In this section, we look deeper at acquisition parameters that exhibit greater variation. We discuss the impact of these existing variations in open datasets. However, empirical quantification of the effect on image quality due to variation in these parameters is out of the scope of this work.

4.1.1 Flip Angle

The flip angle affects the net magnetization relative to the primary magnetic field as it controls the amount of longitudinal magnetization converted to transverse magnetization. Thus, the flip angle affects the RF signal of the cycle, thereby affecting the signal intensity. For instance, large flip angles produce T1 contrast, low flip angles produce PD (proton-density) contrast, and the T1 and PD contrast can cancel each other for intermediate flip angles [37, 38, 39]. Apart from anatomical MRI, the flip angle also affects functional MRI. Large flip angles deteriorate the spatial contrast between cerebrospinal fluid (CSF), gray matter (GM), and white matter (WM), which makes it difficult to align EPI to its structural counterpart [40]. The impact on signal intensity and its significance for pattern discrimination would be governed by specific tissue in context. Yet, it is important to understand that flip angles have a direct effect on image contrast. Figure 5 shows variation in flip angle in field maps for the ABCD dataset.

4.1.2 Echo Time & Repetition Time

A correct choice for echo time (TE) and repetition time (TR) is important for structural images. Acquisition parameters like TR and TE can influence the tissue-specific response as different tissues vary in their respective T1 and T2 times. For instance, to generate a valid T1-weighted image, it is important that the repetition time & echo time is less than tissue-specific T1 & T2 times, respectively. In contrast, repetition time & echo time should be much greater than tissue-specific T1 time & T2 time, respectively, to generate T2-weighted images. However, if repetition time is much greater than tissue-specific T1 time but echo time is less than tissue-specific T2 time, the result is a proton density-weighted image. Thus, variations in repetition time and echo time can dictate image contrast characteristics [17].

Apart from structural images, choice of TR and TE also affects fMRI images. Longer TE values lead to increased susceptibility artifacts and signal dropout. Shorter TRs provide enhanced BOLD senstivity but may also lead to saturation effects [41, 42, 43]

Figure 3 and Figure 6 show the variance of repetition time and echo time for the ABCD dataset and OpenNeuro datasets, respectively.

4.1.3 Magnetic Field Strength

Variation in magnetic field strength has a strong influence on texture features (*e.g.*, co-occurence matrix and gray-level run length matrix). These texture features capture patterns and provide valuable information about visual appearance and structural characteristics of an image. These texture features can significantly impact the performance of predictive models.

Ammari et. al [44] show a comprehensive analysis studying the impact of magnetic field strength on various texture features. The study evaluates 38 texture features of which 15 features in healthy volunteers were sensitive to variations in magnetic field strength. Visually, images from various field strengths may have the same visual diagnostic accuracy [45],

but in context to texture features, images with varying magnetic field strength cannot be used interchangeably [44]. For example, StandardRat dataset (`ds004116`) is a multi-center rat study that contains resting-state fMRI data pooled across 21 datasets. The magnetic field strength varies (4.7 T - 17.15 T) across various scans. Similarly, the magnetic field strength in another multi-center rat dataset `ds004114` varies in the range (3 T - 14.1 T). Careful post-processing techniques should be used to correct for changes in the magnetic field, and failure to correct for these changes can lead to errors and potentially misleading results.

4.1.4 Phase Encoding Direction

PED plays a crucial role in EPI sequences. A common issue in EPI sequences is their vulnerability to artifacts like eddy current effects, off-resonance, and susceptibility artifacts. These artifacts are apparent, especially when the bandwidth is low [46, 47]. To diminish the effect of these distortions, the collection of additional scans with varying PED is very helpful [32]. Although it is important to eliminate these artifacts to improve image quality in DTI sequences, varying the PED is known to affect fractional anisotropy estimates. Kennis et. al [20] show that magnitude of fractional anisotropy magnitude between P$\gg$A and A$\gg$P scans can range from 0.4% to 30% even after correction for subject motion, eddy currents effects, and susceptibility artifacts. It is possible that these differences are arising due to signal intensities from P$\gg$A and A$\gg$P scans that can confound DTI neuroanatomical studies. Similarly, Tudela et. al [48] show that misalignment in PED from the main magnetic field can lead to much more artifacts reflected by lower fractional anisotropy values. Figure 6 shows a histogram to visualize the apportionment of PED for `ds004215` and `ds000201` datasets. The PED should be defined on the specific imaging needs of the subject [20]. However, consistency of PED across subjects can help improve the reliability and accuracy of downstream analyses.

4.2 Effect on statistical analyses

Prior works have measured the effect of various acquisition protocols on texture analysis [49, 50, 51], to evaluate which features are stable against changes in acquisition protocols. Some parameters such as TR and TE do not affect the shape and size of the image, but they affect uniformity in grayscale intensity [21]. It is evident that different acquisition protocols can affect data distribution, reducing the reliability of the extracted features and consequently increasing the bias of downstream statistical analyses [52]. Thus, special attention must be attributed to image pre-processing before any feature extraction [53]. Harmonization is possible only if we know that the data exhibits heterogeneity in imaging acquisition protocol. In cases when sources of non-compliance are not known, data cannot be categorized into clusters, and it would be difficult to perform data harmonization. Thus, *mrQA* can play a pivotal role in establishing data integrity by discovering sources of non-compliance allowing the investigators to perform harmonization, if required. As we progress towards algorithms that are able to learn features automatically (e.g. deep learning), it is even more important to ensure that the derived image features are stable with respect to variations in acquisition parameters [21]. Without acknowledging these sources of variation in acquisition parameters, the statistical results might be subject to confounding which can obscure or exaggerate the effects of interest [54], leading to misinterpretation of statistical results.

4.3 Impact of scanner vendor heterogeneity

Although MRI scanners from different vendors function on the same underlying principles, image sequences can have significant differences in gradient strengths, RF pulse sequences, and timing parameters [55]. In addition, each vendors uses different software and methods to reconstruct the images from k-space. Therefore, these sequences are denoted with specific names and abbreviations. For example, Siemens scanners provide an MPRAGE [56] imaging sequence, while Philips scanners provide SPACE [57] imaging sequence. Both these sequences are T1-weighted images, however significant differences in hardware and software make it non-trivial to compare scans across vendors due to vendor-specific differences in image quality and appearance [58]. It is better to stratify scans w.r.t. a vendor to avoid any misinterpretations. This problem becomes particularly relevant for studies that acquire scans with different imaging acquisition protocols (multi-site studies). Therefore, the subjects are stratified into different vendor-specific sub-groups in Table 2 as per the information in the DICOM header.

We observed that scanners from various vendors (e.g. Siemens, GE, Philips) differ in terms of units of measurement even for the same parameter. For example, in a Siemens scanner, TR is typically in the range of 2000-4000 ms, while the range is typically 6-7.5 ms for a Philips scanner as shown in Figure 3 [5]. The precise details of these differences are stored in Exam Card (Philips), Protocol Exchange (GE), or .exar file (Siemens) generated by corresponding software. These electronic protocol files can be loaded into the corresponding scanner to achieve uniformity of imaging protocol. However, automatic cross-vendor compliance is very difficult due to the lack of standardized open-source tools that can effectively read/write and convert proprietary formats from different vendors.

4.4 Limitations

Although variation in image acquisition parameters can be a source of inconsistencies, an adjustment might be necessary for clinical diagnosis. For instance, high SAR sequences (e.g. FLAIR) for adolescents may be acquired with a slower acquisition time to reduce discomfort in case the SAR limits are exceeded [36]. Furthermore, multiple scans with varying PEDs might be acquired to alleviate susceptibility artifacts [46], or shimming method might be adjusted specifically for a subject to obtain high-quality MRI images [59]. Nevertheless, these variations lead to issues in morphometric estimates [52]. It is possible to include such requirements before analyzing data for protocol compliance by skipping particular parameters known to exhibit high variance. However, the current framework doesn't include this functionality explicitly.

mrQA checks for absolute equivalence for parameter values, that is *mrQA* marks a subject as non-compliant even if there are minor deviations from the reference protocol in any of its runs in a single parameter. However, a standard for compliance is determined by the study design and minor differences in acquisition parameters may not necessarily mean discarding the subjects from the project. Given some context about the study design, it might be possible to include tolerance in these parameters as shown in Figure 4. The standard for acquisition can be best judged by investigators [60, 61] and hence, cannot be attributed prematurely in the software.

mrQA extracts certain acquisition parameters such as the shimming method, effective echo spacing, iPAT, PED, and multi-slice mode from Siemens private headers. All other parameters were extracted using the standard DICOM tags. The current framework skips the private header while reading DICOM images from other scanners such as GE and Philips. Therefore, *mrQA* at its current stage of development cannot discover non-compliance in parameters present in private headers for GE and Philips scanners.

As of now, *mrQA* checks for compliance in a subset of acquisition parameters (in DICOM header) as shown in Table 1. *mrQA* does not validate other potential sources of non-compliance such as scanner software version, slice timing, inversion time, and other sequence specifications present in the DICOM header [62]. Although, this is not necessarily a limitation in itself, as the goal of this exploration is to demonstrate automated protocol compliance. *mrQA* (and *MRdataset*) is fully extensible and we plan to include more acquisition parameters. As more acquisition parameters are incorporated, the percentage of non-compliance is likely to increase, which could further highlight the need to develop strategies for minimizing non-compliance. Nonetheless, the current analysis provides a crucial first step in raising awareness of the prevalence of non-compliance and highlighting the need for improved standardization and reporting in MRI research.

Note that even the DICOM header doesn't contain information about the neuroimaging experiment beyond the specifications of the MR scanner. For instance, a visual stimulus is often used to elicit specific neural responses from various parts of the brain in fMRI analysis. The presentation of stimuli can vary across sites due to differences in their duration, and intensity; which may in turn affect the measurement of neural responses. Consequently, differences in neural responses would make it difficult to pool and interpret data across scanners. Similarly, it is essential to retain reactivity measurements such as CO2 inhalation, acetazolamide infusion *etc*.,However, these measurements are not exported from the scanner in standard DICOM tags [63]. Therefore checking compliance in the DICOM header may not be sufficient to achieve consistent acquisition across multiple sites.

5 Conclusions

We demonstrate the pervasive problem of protocol non-compliance based on analyses of many open datasets from OpenNeuro and the ABCD dataset. It is non-trivial to maintain protocol compliance in imaging acquisition parameters, especially for large-scale multi-site studies. Insufficient monitoring can lead to non-compliance in MR physics parameters which may confound downstream statistical analyses. Therefore, we propose an open-source tool, *mrQA* (and *MRdataset*) which can summarize and aggregate acquisition parameters to discover any issues of protocol non-compliance. Apart from generating compliance reports, mrQA can be set up for continuous monitoring of acquired DICOM images on a daily/weekly basis. We believe that it is important to embrace a mindset of proactive quality assurance to weed out any source of inconsistencies at the scanning interface itself rather than waiting for the end-of-analyses to catch confounding. Adopting such an approach before organizing files in a suitable directory structure (e.g. BIDS) will save time and effort. The long-term goal is to analyze DICOM images in near real-time to identify and fix any issues of non-compliance at the scanner itself. As we move towards even larger datasets, automated imaging QA would be critical for dataset integrity and valid statistical analyses. *mrQA* can help automate this process, as we move towards practical, efficient, and potentially real-time monitoring of protocol compliance.

Acknowledgments

We would also like to thank Drs. Ashok Panigrahy, Beatriz Luna, Claudiu Schirda, Chan-Hong Moon, Tae Kim, Victor Yushmanov, Andrew Reineberg, and Yaroslav Halchenko for their comments and helpful discussions. We would like to thank Tanupat Boonchalermvichien for his software contributions to the parsing DICOM format. We are grateful to the Pittsburgh Supercomputing Center and the XSEDE initiative for providing computational resources for this work. Harsh Sinha is supported by the Intelligent Systems Program Fellowship from the University of Pittsburgh.

References

[1] Peter A. Bandettini. Twenty years of functional MRI: The science and the stories. *NeuroImage*, 62(2):575–588, August 2012. ISSN 10538119. doi:10.1016/j.neuroimage.2012.04.026.

[2] Denes Szucs and John PA. Ioannidis. Sample size evolution in neuroimaging research: An evaluation of highly-cited studies (1990–2012) and of latest practices (2017–2018) in high-impact journals. *NeuroImage*, 221:117164, November 2020. ISSN 10538119. doi:10.1016/j.neuroimage.2020.117164.

[3] R. C. Petersen, P. S. Aisen, L. A. Beckett, M. C. Donohue, A. C. Gamst, D. J. Harvey, C. R. Jack, W. J. Jagust, L. M. Shaw, A. W. Toga, J. Q. Trojanowski, and M. W. Weiner. Alzheimer's Disease Neuroimaging Initiative (ADNI): Clinical characterization. *Neurology*, 74(3):201–209, January 2010. ISSN 0028-3878, 1526-632X. doi:10.1212/WNL.0b013e3181cb3e25.

[4] David C. Van Essen, Stephen M. Smith, Deanna M. Barch, Timothy E.J. Behrens, Essa Yacoub, and Kamil Ugurbil. The WU-Minn Human Connectome Project: An overview. *NeuroImage*, 80:62–79, October 2013. ISSN 10538119. doi:10.1016/j.neuroimage.2013.05.041.

[5] B.J. Casey, Tariq Cannonier, May I. Conley, Alexandra O. Cohen, Deanna M. Barch, Mary M. Heitzeg, Mary E. Soules, Theresa Teslovich, Danielle V. Dellarco, Hugh Garavan, Catherine A. Orr, Tor D. Wager, Marie T. Banich, Nicole K. Speer, Matthew T. Sutherland, Michael C. Riedel, Anthony S. Dick, James M. Bjork, Kathleen M. Thomas, Bader Chaarani, Margie H. Mejia, Donald J. Hagler, M. Daniela Cornejo, Chelsea S. Sicat, Michael P. Harms, Nico U.F. Dosenbach, Monica Rosenberg, Eric Earl, Hauke Bartsch, Richard Watts, Jonathan R. Polimeni, Joshua M. Kuperman, Damien A. Fair, and Anders M. Dale. The Adolescent Brain Cognitive Development (ABCD) study: Imaging acquisition across 21 sites. *Developmental Cognitive Neuroscience*, 32:43–54, August 2018. ISSN 18789293. doi:10.1016/j.dcn.2018.03.001.

[6] Jorge Jovicich, Silvester Czanner, Xiao Han, David Salat, Andre van der Kouwe, Brian Quinn, Jenni Pacheco, Marilyn Albert, Ronald Killiany, and Deborah Blacker. MRI-derived measurements of human subcortical, ventricular and intracranial brain volumes: Reliability effects of scan sessions, acquisition sequences, data analyses, scanner upgrade, scanner vendors and field strengths. *NeuroImage*, 46(1):177–192, May 2009. ISSN 10538119. doi:10.1016/j.neuroimage.2009.02.010.

[7] Lee Friedman, Hal Stern, Gregory G. Brown, Daniel H. Mathalon, Jessica Turner, Gary H. Glover, Randy L. Gollub, John Lauriello, Kelvin O. Lim, Tyrone Cannon, Douglas N. Greve, Henry Jeremy Bockholt, Aysenil Belger, Bryon Mueller, Michael J. Doty, Jianchun He, William Wells, Padhraic Smyth, Steve Pieper, Seyoung Kim, Marek Kubicki, Mark Vangel, and Steven G. Potkin. Test-retest and between-site reliability in a multicenter fMRI study. *Human Brain Mapping*, 29(8):958–972, August 2008. ISSN 10659471. doi:10.1002/hbm.20440.

[8] Sylvain Gouttard, Martin Styner, Marcel Prastawa, Joseph Piven, and Guido Gerig. Assessment of Reliability of Multi-site Neuroimaging Via Traveling Phantom Study. *Springer*, 5242:263–270, September 2008. doi:10.1007/978-3-540-85990-1_32. Series Title: Lecture Notes in Computer Science.

[9] Jorge Jovicich, Silvester Czanner, Douglas Greve, Elizabeth Haley, Andre van der Kouwe, Randy Gollub, David Kennedy, Franz Schmitt, Gregory Brown, James MacFall, Bruce Fischl, and Anders Dale. Reliability in multi-site structural MRI studies: Effects of gradient non-linearity correction on phantom and human data. *NeuroImage*, 30 (2):436–443, April 2006. ISSN 10538119. doi:10.1016/j.neuroimage.2005.09.046.

[10] Heath Pardoe, Gaby S. Pell, David F. Abbott, Anne T. Berg, and Graeme D. Jackson. Multi-site voxel-based morphometry: Methods and a feasibility demonstration with childhood absence epilepsy. *NeuroImage*, 42(2): 611–616, August 2008. ISSN 10538119. doi:10.1016/j.neuroimage.2008.05.007.

[11] Hugo G. Schnack, Neeltje E.M. van Haren, Hilleke E. Hulshoff Pol, Marco Picchioni, Matthias Weisbrod, Heinrich Sauer, Tyrone Cannon, Matti Huttunen, Robin Murray, and Ren S. Kahn. Reliability of brain volumes from multicenter MRI acquisition: A calibration study. *Human Brain Mapping*, 22(4):312–320, August 2004. ISSN 1065-9471, 1097-0193. doi:10.1002/hbm.20040.

[12] Jean-Philippe Fortin, Nicholas Cullen, Yvette I. Sheline, Warren D. Taylor, Irem Aselcioglu, Philip A. Cook, Phil Adams, Crystal Cooper, Maurizio Fava, Patrick J. McGrath, Melvin McInnis, Mary L. Phillips, Madhukar H. Trivedi, Myrna M. Weissman, and Russell T. Shinohara. Harmonization of cortical thickness measurements across scanners and sites. *NeuroImage*, 167:104–120, February 2018. ISSN 10538119. doi:10.1016/j.neuroimage.2017.11.024.

[13] Allan George, Ruben Kuzniecky, Henry Rusinek, Heath R. Pardoe, and for the Human Epilepsy Project Investigators. Standardized Brain MRI Acquisition Protocols Improve Statistical Power in Multicenter Quantitative Morphometry Studies. *Journal of Neuroimaging*, 30(1):126–133, January 2020. ISSN 1051-2284, 1552-6569. doi:10.1111/jon.12673.

[14] Clifford R. Jack, Matt A. Bernstein, Nick C. Fox, Paul Thompson, Gene Alexander, Danielle Harvey, Bret Borowski, Paula J. Britson, Jennifer L. Whitwell, Chadwick Ward, Anders M. Dale, Joel P. Felmlee, Jeffrey L. Gunter, Derek L.G. Hill, Ron Killiany, Norbert Schuff, Sabrina Fox-Bosetti, Chen Lin, Colin Studholme, Charles S. DeCarli, Gunnar Krueger, Heidi A. Ward, Gregory J. Metzger, Katherine T. Scott, Richard Mallozzi, Daniel Blezek, Joshua Levy, Josef P. Debbins, Adam S. Fleisher, Marilyn Albert, Robert Green, George Bartzokis, Gary Glover, John Mugler, Michael W. Weiner, and ADNI Study. The Alzheimer's disease neuroimaging initiative (ADNI): MRI methods. *Journal of Magnetic Resonance Imaging*, 27(4):685–691, April 2008. ISSN 10531807, 15222586. doi:10.1002/jmri.21049.

[15] G. Pearlson. Multisite Collaborations and Large Databases in Psychiatric Neuroimaging: Advantages, Problems, and Challenges. *Schizophrenia Bulletin*, 35(1):1–2, January 2009. ISSN 0586-7614, 1745-1701. doi:10.1093/schbul/sbn166.

[16] Katherine S. Button, John P. A. Ioannidis, Claire Mokrysz, Brian A. Nosek, Jonathan Flint, Emma S. J. Robinson, and Marcus R. Munafò. Power failure: why small sample size undermines the reliability of neuroscience. *Nature Reviews Neuroscience*, 14(5):365–376, May 2013. ISSN 1471-003X, 1471-0048. doi:10.1038/nrn3475.

[17] Garry E. Gold, Eric Han, Jeff Stainsby, Graham Wright, Jean Brittain, and Christopher Beaulieu. Musculoskeletal MRI at 3.0 T: Relaxation Times and Image Contrast. *American Journal of Roentgenology*, 183(2):343–351, August 2004. ISSN 0361-803X, 1546-3141. doi:10.2214/ajr.183.2.1830343.

[18] Peter Jezzard and Robert S. Balaban. Correction for geometric distortion in echo planar images from B0 field variations. *Magnetic Resonance in Medicine*, 34(1):65–73, July 1995. ISSN 07403194, 15222594. doi:10.1002/mrm.1910340111.

[19] Peter Jezzard. Correction of geometric distortion in fMRI data. *NeuroImage*, 62(2):648–651, August 2012. ISSN 10538119. doi:10.1016/j.neuroimage.2011.09.010.

[20] M. Kennis, S.J.H. van Rooij, R.S. Kahn, E. Geuze, and A. Leemans. Choosing the polarity of the phase-encoding direction in diffusion MRI: Does it matter for group analysis? *NeuroImage: Clinical*, 11:539–547, 2016. ISSN 22131582. doi:10.1016/j.nicl.2016.03.022.

[21] Marius E. Mayerhoefer, Pavol Szomolanyi, Daniel Jirak, Andrzej Materka, and Siegfried Trattnig. Effects of MRI acquisition parameter variations and protocol heterogeneity on the results of texture analysis and pattern discrimination: An application-oriented study: Effects of MRI acquisition parameters on texture analysis. *Medical Physics*, 36(4):1236–1243, March 2009. ISSN 00942405. doi:10.1118/1.3081408.

[22] Daniel R. Glen, Paul A. Taylor, Bradley R. Buchsbaum, Robert W. Cox, and Richard C. Reynolds. Beware (Surprisingly Common) Left-Right Flips in Your MRI Data: An Efficient and Robust Method to Check MRI Dataset Consistency Using AFNI. *Frontiers in Neuroinformatics*, 14:18, May 2020. ISSN 1662-5196. doi:10.3389/fninf.2020.00018.

[23] Sydney Covitz, Tinashe M. Tapera, Azeez Adebimpe, Aaron F. Alexander-Bloch, Maxwell A. Bertolero, Eric Feczko, Alexandre R. Franco, Raquel E. Gur, Ruben C. Gur, Timothy Hendrickson, Audrey Houghton, Kahini Mehta, Kristin Murtha, Anders J. Perrone, Tim Robert-Fitzgerald, Jenna M. Schabdach, Russell T Shinohara, Jacob W. Vogel, Chenying Zhao, Damien A. Fair, Michael P. Milham, Matthew Cieslak, and Theodore D. Satterthwaite. Curation of bids (cubids): A workflow and software package for streamlining reproducible curation of large bids datasets. *NeuroImage*, 263:119609, Nov 2022. ISSN 10538119. doi:10.1016/j.neuroimage.2022.119609.

[24] Terry L Jernigan. Adolescent Brain Cognitive Development Study (ABCD), January 2017.

[25] Christopher J Markiewicz, Krzysztof J Gorgolewski, Franklin Feingold, Ross Blair, Yaroslav O Halchenko, Eric Miller, Nell Hardcastle, Joe Wexler, Oscar Esteban, Mathias Goncavles, Anita Jwa, and Russell Poldrack. The openneuro resource for sharing of neuroscience data. *eLife*, 10:e71774, Oct 2021. ISSN 2050-084X. doi:10.7554/eLife.71774.

[26] Kenneth Clark, Bruce Vendt, Kirk Smith, John Freymann, Justin Kirby, Paul Koppel, Stephen Moore, Stanley Phillips, David Maffitt, Michael Pringle, Lawrence Tarbox, and Fred Prior. The Cancer Imaging Archive (TCIA): Maintaining and Operating a Public Information Repository. *Journal of Digital Imaging*, 26(6):1045–1057, December 2013. ISSN 0897-1889, 1618-727X. doi:10.1007/s10278-013-9622-7.

[27] Martin A Lindquist and Tor D Wager. *Principles of functional Magnetic Resonance Imaging*. London: CRC Press, July 2015.

[28] Darcy Mason, Scaramallion, Mrbean-Bremen, Rhaxton, Jonathan Suever, Vanessasaurus, Dimitri Papadopoulos Orfanos, Guillaume Lemaitre, Aditya Panchal, Alex Rothberg, Markus D. Herrmann, Joan Massich, James Kerns, Korijn Van Golen, Thomas Robitaille, Simon Biggs, Moloney, Chris Bridge, Matthew Shun-Shin, Blair Conrad, Pawelzajdel, Markus Mattes, YoungKi Lyu, Félix C. Morency, Tim Cogan, Bernardo Pericacho Sánchez, Hans Meine, Joseph Wortmann, Kevin S. Hahn, and Masahiro Wada. pydicom/pydicom: pydicom 2.3.1, November 2022.

[29] Pradeep Raamana. Let's focus our neuroinformatics community efforts in Python and on software validation, May 2018.

[30] Peter B Barker, Alberto Bizzi, Nicola De Stefano, Doris DM Lin, and Rao Gullapalli. *Clinical MR spectroscopy: techniques and applications*. Cambridge University Press, 2010. ISBN 978-0-521-86898-3.

[31] Betty Jo Casey, Tariq Cannonier, May I Conley, Alexandra O Cohen, Deanna M Barch, Mary M Heitzeg, Mary E Soules, Theresa Teslovich, Danielle V Dellarco, Hugh Garavan, et al. The adolescent brain cognitive development (abcd) study: imaging acquisition across 21 sites. *Developmental cognitive neuroscience*, 32:43–54, 2018.

[32] M. Okan Irfanoglu, Lindsay Walker, Joelle Sarlls, Stefano Marenco, and Carlo Pierpaoli. Effects of image distortions originating from susceptibility variations and concomitant fields on diffusion MRI tractography results. *NeuroImage*, 61(1):275–288, May 2012. ISSN 10538119. doi:10.1016/j.neuroimage.2012.02.054.

[33] Xiangrui Li, Paul S. Morgan, John Ashburner, Jolinda Smith, and Christopher Rorden. The first step for neuroimaging data analysis: DICOM to NIfTI conversion. *Journal of Neuroscience Methods*, 264:47–56, May 2016. ISSN 01650270. doi:10.1016/j.jneumeth.2016.03.001.

[34] Eric Feczko, Greg Conan, Scott Marek, Brenden Tervo-Clemmens, Michaela Cordova, Olivia Doyle, Eric Earl, Anders Perrone, Darrick Sturgeon, Rachel Klein, et al. Adolescent brain cognitive development (abcd) community mri collection and utilities. *BioRxiv*, pages 2021–07, 2021.

[35] Mark D. Wilkinson, Michel Dumontier, IJsbrand Jan Aalbersberg, Gabrielle Appleton, Myles Axton, Arie Baak, Niklas Blomberg, Jan-Willem Boiten, Luiz Bonino da Silva Santos, Philip E. Bourne, Jildau Bouwman, Anthony J. Brookes, Tim Clark, Mercè Crosas, Ingrid Dillo, Olivier Dumon, Scott Edmunds, Chris T. Evelo, Richard Finkers, Alejandra Gonzalez-Beltran, Alasdair J.G. Gray, Paul Groth, Carole Goble, Jeffrey S. Grethe, Jaap Heringa, Peter A.C 't Hoen, Rob Hooft, Tobias Kuhn, Ruben Kok, Joost Kok, Scott J. Lusher, Maryann E. Martone, Albert Mons, Abel L. Packer, Bengt Persson, Philippe Rocca-Serra, Marco Roos, Rene van Schaik, Susanna-Assunta Sansone, Erik Schultes, Thierry Sengstag, Ted Slater, George Strawn, Morris A. Swertz, Mark Thompson, Johan van der Lei, Erik van Mulligen, Jan Velterop, Andra Waagmeester, Peter Wittenburg, Katherine Wolstencroft, Jun Zhao, and Barend Mons. The FAIR Guiding Principles for scientific data management and stewardship. *Scientific Data*, 3(1):160018, March 2016. ISSN 2052-4463. doi:10.1038/sdata.2016.18.

[36] Jerry Allison and Nathan Yanasak. What MRI Sequences Produce the Highest Specific Absorption Rate (SAR), and Is There Something We Should Be Doing to Reduce the SAR During Standard Examinations? *American Journal of Roentgenology*, 205(2):W140–W140, August 2015. ISSN 0361-803X, 1546-3141. doi:10.2214/AJR.14.14173.

[37] Constantin Sandmann, Erlend Hodneland, and Jan Modersitzki. A practical guideline for T_1 reconstruction from various flip angles in MRI. *Journal of Algorithms & Computational Technology*, 10(4):213–223, December 2016. ISSN 1748-3026, 1748-3026. doi:10.1177/1748301816656288.

[38] Fabien Balezeau, Pierre-Antoine Eliat, Alejandro Bordelois Cayamo, and Hervé Saint-Jalmes. Mapping of low flip angles in magnetic resonance. *Physics in Medicine and Biology*, 56(20):6635–6647, October 2011. ISSN 0031-9155, 1361-6560. doi:10.1088/0031-9155/56/20/008.

[39] G Lutterbey, M P Wattjes, J Kandyba, M Harzheim, M V Falkenhausen, N Morakkabati, H Schild, and J Gieseke. Clinical evaluation of a speed optimized T_2 weighted fast spin echo sequence at 3.0 T using variable flip angle refocusing, half-Fourier acquisition and parallel imaging. *The British Journal of Radiology*, 80(956):668–673, August 2007. ISSN 0007-1285, 1748-880X. doi:10.1259/bjr/88996134.

[40] J. Gonzalez-Castillo, V. Roopchansingh, P.A. Bandettini, and J. Bodurka. Physiological noise effects on the flip angle selection in BOLD fMRI. *NeuroImage*, 54(4):2764–2778, February 2011. ISSN 10538119. doi:10.1016/j.neuroimage.2010.11.020.

[41] Jingyuan E. Chen and Gary H. Glover. Functional magnetic resonance imaging methods. *Neuropsychology Review*, 25(3):289–313, Sep 2015. ISSN 1573-6660. doi:10.1007/s11065-015-9294-9.

[42] David A. Feinberg and Kawin Setsompop. Ultra-fast mri of the human brain with simultaneous multi-slice imaging. *Journal of Magnetic Resonance*, 229:90–100, Apr 2013. ISSN 1090-7807. doi:10.1016/j.jmr.2013.02.002.

[43] Russell A. Poldrack, Paul C. Fletcher, Richard N. Henson, Keith J. Worsley, Matthew Brett, and Thomas E. Nichols. Guidelines for reporting an fmri study. *NeuroImage*, 40(2):409–414, Apr 2008. ISSN 1053-8119. doi:10.1016/j.neuroimage.2007.11.048.

[44] Samy Ammari, Stephanie Pitre-Champagnat, Laurent Dercle, Emilie Chouzenoux, Salma Moalla, Sylvain Reuze, Hugues Talbot, Tite Mokoyoko, Joya Hadchiti, Sebastien Diffetocq, Andreas Volk, Mickeal El Haik, Sara Lakiss, Corinne Balleyguier, Nathalie Lassau, and Francois Bidault. Influence of Magnetic Field Strength on Magnetic Resonance Imaging Radiomics Features in Brain Imaging, an In Vitro and In Vivo Study. *Frontiers in Oncology*, 10:541663, January 2021. ISSN 2234-943X. doi:10.3389/fonc.2020.541663.

[45] Brian K. Rutt and Donald H. Lee. The impact of field strength on image quality in MRI. *Journal of Magnetic Resonance Imaging*, 6(1):57–62, January 1996. ISSN 10531807, 15222586. doi:10.1002/jmri.1880060111.

[46] Derek K. Jones and Mara Cercignani. Twenty-five pitfalls in the analysis of diffusion MRI data. *NMR in Biomedicine*, 23(7):803–820, September 2010. ISSN 09523480. doi:10.1002/nbm.1543.

[47] Denis Le Bihan, Cyril Poupon, Alexis Amadon, and Franck Lethimonnier. Artifacts and pitfalls in diffusion MRI. *Journal of Magnetic Resonance Imaging*, 24(3):478–488, September 2006. ISSN 1053-1807, 1522-2586. doi:10.1002/jmri.20683.

[48] Raúl Tudela, Emma Muñoz-Moreno, Xavier López-Gil, and Guadalupe Soria. Effects of Orientation and Anisometry of Magnetic Resonance Imaging Acquisitions on Diffusion Tensor Imaging and Structural Connectomes. *PLOS ONE*, 12(1):e0170703, January 2017. ISSN 1932-6203. doi:10.1371/journal.pone.0170703.

[49] Alexandre Carré, Guillaume Klausner, Myriam Edjlali, Marvin Lerousseau, Jade Briend-Diop, Roger Sun, Samy Ammari, Sylvain Reuzé, Emilie Alvarez Andres, Théo Estienne, Stéphane Niyoteka, Enzo Battistella, Maria Vakalopoulou, Frédéric Dhermain, Nikos Paragios, Eric Deutsch, Catherine Oppenheim, Johan Pallud, and Charlotte Robert. Standardization of brain MR images across machines and protocols: bridging the gap for MRI-based radiomics. *Scientific Reports*, 10(1):12340, December 2020. ISSN 2045-2322. doi:10.1038/s41598-020-69298-z.

[50] Prathyush Chirra, Patrick Leo, Michael Yim, B. Nicolas Bloch, Ardeshir R. Rastinehad, Andrei Purysko, Mark Rosen, Anant Madabhushi, and Satish E. Viswanath. Multisite evaluation of radiomic feature reproducibility and discriminability for identifying peripheral zone prostate tumors on MRI. *Journal of Medical Imaging*, 6(02):1, June 2019. ISSN 2329-4302. doi:10.1117/1.JMI.6.2.024502.

[51] Marco Bologna, Valentina Corino, and Luca Mainardi. Technical Note: Virtual phantom analyses for preprocessing evaluation and detection of a robust feature set for MRI-radiomics of the brain. *Medical Physics*, 46(11):5116–5123, November 2019. ISSN 0094-2405, 2473-4209. doi:10.1002/mp.13834.

[52] Niels W. Schurink, Simon R. van Kranen, Sander Roberti, Joost J. M. van Griethuysen, Nino Bogveradze, Francesca Castagnoli, Najim el Khababi, Frans C. H. Bakers, Shira H. de Bie, Gerlof P. T. Bosma, Vincent C. Cappendijk, Remy W. F. Geenen, Peter A. Neijenhuis, Gerald M. Peterson, Cornelis J. Veeken, Roy F. A. Vliegen, Regina G. H. Beets-Tan, and Doenja M. J. Lambregts. Sources of variation in multicenter rectal MRI data and their effect on radiomics feature reproducibility. *European Radiology*, 32(3):1506–1516, March 2022. ISSN 0938-7994, 1432-1084. doi:10.1007/s00330-021-08251-8.

[53] Yingping Li, Samy Ammari, Corinne Balleyguier, Nathalie Lassau, and Emilie Chouzenoux. Impact of Preprocessing and Harmonization Methods on the Removal of Scanner Effects in Brain MRI Radiomic Features. *Cancers*, 13(12):3000, June 2021. ISSN 2072-6694. doi:10.3390/cancers13123000.

[54] Robert Geirhos, Jörn-Henrik Jacobsen, Claudio Michaelis, Richard Zemel, Wieland Brendel, Matthias Bethge, and Felix A. Wichmann. Shortcut learning in deep neural networks. *Nature Machine Intelligence*, 2(1111):665–673, Nov 2020. ISSN 2522-5839. doi:10.1038/s42256-020-00257-z.

[55] T. Okada, M. Kanagaki, A. Yamamoto, R. Sakamoto, S. Kasahara, E. Morimoto, M. Iima, T. M. Mehemed, S. Nakajima, and K. and Togashi. Which to choose for volumetry: MPRAGE or SPACE? In *2011 ISMRM Annual Meeting and Exhibition (ISMRM)*, Quebec, Canada, April 2011. ISMRM.

[56] John P. Mugler. Optimized three-dimensional fast-spin-echo mri. *ISMRM Annual Meeting and Exhibition*, 39(4):745–767, May 2011. ISSN 1053-1807, 1522-2586. doi:10.1002/jmri.24542.

[57] Jaeseok Park, John P. Mugler, Wilhelm Horger, and Berthold Kiefer. OptimizedT1-weighted contrast for single-slab 3D turbo spin-echo imaging with long echo trains: Application to whole-brain imaging. *Magnetic Resonance in Medicine*, 58(5):982–992, November 2007. ISSN 07403194, 15222594. doi:10.1002/mrm.21386.

[58] Stephen S F Yip and Hugo J W L Aerts. Applications and limitations of radiomics. *Physics in Medicine and Biology*, 61(13):R150–R166, July 2016. ISSN 0031-9155, 1361-6560. doi:10.1088/0031-9155/61/13/R150.

[59] Rolf Gruetter. Automatic, localizedin Vivo adjustment of all first-and second-order shim coils. *Magnetic Resonance in Medicine*, 29(6):804–811, June 1993. ISSN 07403194, 15222594. doi:10.1002/mrm.1910290613.

[60] Céline Provins, Eilidh MacNicol, Saren H. Seeley, Patric Hagmann, and Oscar Esteban. Quality control in functional MRI studies with MRIQC and fMRIPrep. *Frontiers in Neuroimaging*, 1:1073734, January 2023. ISSN 2813-1193. doi:10.3389/fnimg.2022.1073734.

[61] Richard C. Reynolds, Paul A. Taylor, and Daniel R. Glen. Quality control practices in FMRI analysis: Philosophy, methods and examples using AFNI. *Frontiers in Neuroscience*, 16:1073800, January 2023. ISSN 1662-453X. doi:10.3389/fnins.2022.1073800.

[62] Ben Inglis. A checklist for fMRI acquisition methods reporting in the literature. *The Winnower*, 2015. ISSN 2373-146X. doi:10.15200/winn.143191.17127.

[63] Patricia Clement, Marco Castellaro, Thomas W. Okell, David L. Thomas, Pieter Vandemaele, Sara Elgayar, Aaron Oliver-Taylor, Thomas Kirk, Joseph G. Woods, Sjoerd B. Vos, Joost P. A. Kuijer, Eric Achten, Matthias J. P. van Osch, John A. Detre, Hanzhang Lu, David C. Alsop, Michael A. Chappell, Luis Hernandez-Garcia, Jan Petr, and Henk J. M. M. Mutsaerts. Asl-bids, the brain imaging data structure extension for arterial spin labeling. *Scientific Data*, 9(11):543, Sep 2022. ISSN 2052-4463. doi:10.1038/s41597-022-01615-9.

[64] Lisa Scarpace, Adam E. Flanders, Rajan Jain, Tom Mikkelsen, and David W. Andrews. Data From REMBRANDT, 2019. Version Number: 2 Type: dataset.

[65] Lisa Scarpace, Tom Mikkelsen, Soonmee Cha, Sujaya Rao, Sangeeta Tekchandani, David Gutman, Joel H. Saltz, Bradley J. Erickson, Nancy Pedano, Adam E. Flanders, Jill Barnholtz-Sloan, Quinn Ostrom, Daniel Barboriak, and Laura J. Pierce. The Cancer Genome Atlas Glioblastoma Multiforme Collection (TCGA-GBM), 2016. Version Number: 4 Type: dataset.

[66] Nancy Pedano, Adam E. Flanders, Lisa Scarpace, Tom Mikkelsen, Jennifer M. Eschbacher, Beth Hermes, Victor Sisneros, Jill Barnholtz-Sloan, and Quinn Ostrom. The Cancer Genome Atlas Low Grade Glioma Collection (TCGA-LGG), 2016. Version Number: 3 Type: dataset.

A Evaluation of DICOM datasets on TCIA

Although we focus primarily on neuroimaging datasets, *mrQA* can analyze DICOM-based datasets for other organs also. We also analyze three public DICOM datasets available on The Cancer Imaging Archive (TCIA) [26], namely Rembrandt [64], TCGA-GBM [65] and TCGA-LGG [66]. For Rembrandt, we observe issues of non-compliance in TR. Many scans had missing values for crucial parameters like magnetic field strength, pixel bandwidth, PED for FLAIR, and diffusion images. We observe issues in repetition time, pixel bandwidth, and magnetic field strength for TCGA-LGG and TCGA-GBM datasets. Missing acquisition parameters can not only limit reproducibility, it also limits the ability to perform comparative analysis across studies, which consequently affects the validity and reliability of the research. The compliance reports for TCIA are available at https://github.com/Open-Minds-Lab/mrQA-reports